Lasers in Manufacturing Conference 2015

Simulation of the effect of different laser beam intensity profiles on heat distribution in selective laser melting

Tim Marten Wischeropp[1]*, Raul Salazar[1], Dirk Herzog[2], Claus Emmelmann[2]

[a]*Institute of Laser and System Technologies, Denickestr. 17, 21073 Hamburg, Germany*
[b]*LZN Laser Zentrum Nord GmbH, Am Schleusengraben 14, 21029 Hamburg, Germany*

Abstract

The application of Additive Manufacturing technologies is rapidly increasing. Despite the numerous advantages, one of the major shortcomings is the comparable low productivity of the process. An optimized laser beam intensity profile promises a more uniform energy input, increased energy efficiency, reduced vaporization and therefore an increase in melting rate and productivity.
This paper presents a 2D-FEM model, which qualitatively simulates the heat distribution for the melting of TiAl6V4 powder on top of a solid TiAl6V4 block in an efficient way. With the help of the model, the heat distribution during the melting of a single track was simulated for three different laser beam intensity profiles as well as scanning speeds and laser powers. The results show a significant increase in energy efficiency as well as lower amount of vaporized material for donut shaped laser beam intensity profiles in comparison to Gaussian ones, promising higher build-up rates.

Keywords: Additive Manufacturing, Fundamentals and Process Simulation, Beam Shaping

1. Introduction

Selective Laser Melting (SLM) is a layer-wise Rapid Manufacturing technology capable of manufacturing fully-dense and high quality metal-parts by utilizing a focused laser beam to melt and solidify a powder material according to the corresponding 3D-CAD model. Due to the numerous advantages of SLM compared to conventional manufacturing technologies, its application has been rapidly increasing with currently double digit growth figures, as shown in Wohlers, 2014. Although serial production has already been realized

* Corresponding author. Tel.: +49-40-48-40-10-722; fax: +49-40-48-40-10-777.
E-mail address: tim.wischeropp@tuhh.de.

for several components, large batch production is not profitable in many cases. The low productivity of the SLM-machines and hence high manufacturing costs are one of the main reasons. Consequently, increasing productivity is crucial in order to extend the area of application for SLM in serial production.

The most recent increase in productivity of the SLM-process was achieved by using up to four lasers at the same time and by implementing the hull-core scanning strategy. Unfortunately the limited installation space for optical components hinders a further increase in the number of lasers used and the hull-core strategy only offers significant benefits to parts with comparable heavy wall-thickness, usually not manufactured with SLM. Therefore it is necessary to work on alternative options to increase the productivity.

The productivity of a single laser source in the SLM process is limited by the maximum energy input, which depends on material properties as well as process parameters. The Gaussian laser beam intensity profile, most commonly used in SLM-machines, leads to an imbalanced temperature distribution. Although it has been shown for other laser material processes such as laser metal deposition (Giuliani et al., 2009) and laser hardening (Wellburn et al., 2014) that process optimization is feasible by optimizing the laser beam intensity profile, no profound research on the effect for SLM has been done so far.

To simulate the effect different laser beam intensity profiles have on the energy input and heat distribution during the process, an FEM model considering the thermal effects during the SLM-process was developed.

2. Development of the FEM Model

Various FEM models for the simulation of the SLM process have been developed in the past years to understand the interaction of a laser beam with the powder bed (e.g. Zeng et al., 2012), to calculate the residual stresses in a part (e.g. Zaeh and Branner, 2009) or to predefine scanning parameters (e.g. Song et al., 2011). Recent studies investigated the influence different laser beam intensity profiles have on residual stresses in stainless steel (Cloots et al., 2013), but there is a lack of investigations on how the energy input and heat distribution can be optimized by alternative laser beam intensity profiles.

For a first investigation on this topic, it is necessary to get a basic understanding on how different laser beam intensity profiles affect the energy input and heat distribution in SLM. Therefore an FEM model was developed, capable of effectively simulating the heat distribution on a qualitative basis. To reduce the complexity of the model and hence the computation time, the model focuses on simulating the thermal heat distribution, neglecting any mechanical effects.

2.1. Comparison of 2D- and 3D-simulation

From Vansteenkiste, 2012, it is known that a 2D-simulation of the transversal plane, as shown in figure 1, is capable of simulating heat transfer in SLM accurately and reduces the computation time up to a factor of 20. When modeling the interaction of different laser beam intensity profiles during the SLM process, the mesh sizes has to be much finer then the beam radius to accurately define the intensity profiles (refer to figure 2), leading to massive computation time in 3D. Hence a 2D-simulation would be favorable.

To confirm the assumption that a 2D-model can simulate the heat transfer mechanisms in SLM accurately, a Gaussian laser beam scanning on top of a solid block of TiAl6V4 was simulated in a 2D- and 3D-model. The 2D-model represents a cross section of the bulk material, as shown in figure 1. For a constant laser power P_L the corresponding width of the melt-pool was measured for different scanning speeds v_S. The parameters used for the simulation are listed in table 1.

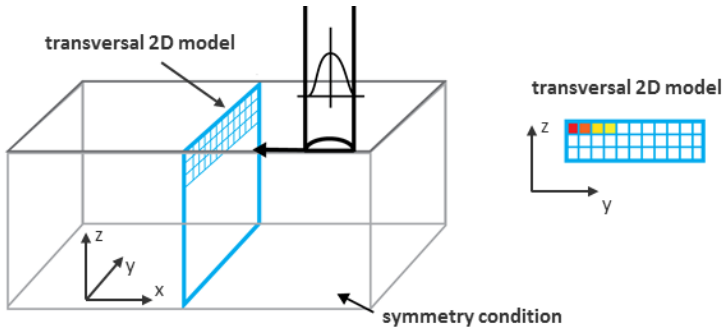

Fig. 1. Basic setup of the 2D- and 3D-FEM model

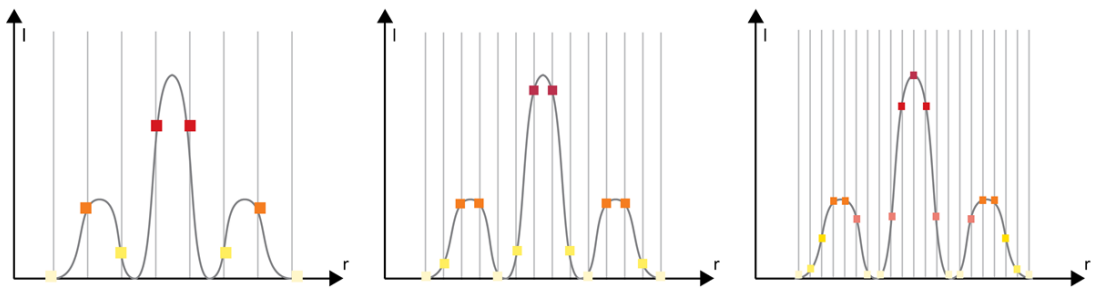

Fig. 2. Definition of laser beam intensity profile in relation to mesh size.

Table 1. Parameters for the comparison of 2D- and 3D-simulation

Parameter	Value	Unit
Solid absorption	40	%
Liquid absorption	40	%
Laser beam radius	45	µm
Laser power P_L	180	W
Scanning speed v_S	500, 700, 900, 1100, 1300, 1500	mm/s
Laser beam intensity profile	Gaussian	
Material Properties	TiAl6V4 bulk material; refer to chapter 2.3	

As can be seen from the results in figure 3, the size of the melt-pool for the 2D-simulation is constantly higher than the one of the 3D-simulation. Additionally, it can be seen that for high scanning speeds (>900 mm/s) the results of the 2D- and 3D-simulation are in good agreement, exemplarily shown in figure 4. This can be explained by the absence of heat conduction in x-direction in the 2D-model and by the fact that for high scanning speeds the heat conduction in x-direction has minor influence. For simulations with powder material, the difference between 2D- and 3D-simulation will be even smaller due to the very low conductivity of the powder material, which varies between 1% of the corresponding value of the bulk material in Gusarov et al., 2009, up to a value, where the conductivity of the bulk material is reduced by the porosity of the powder as in Roberts et al., 2009. Therefore one could state, that for high scanning speeds a 2D-model can be used to efficiently predict heat distribution during the SLM process.

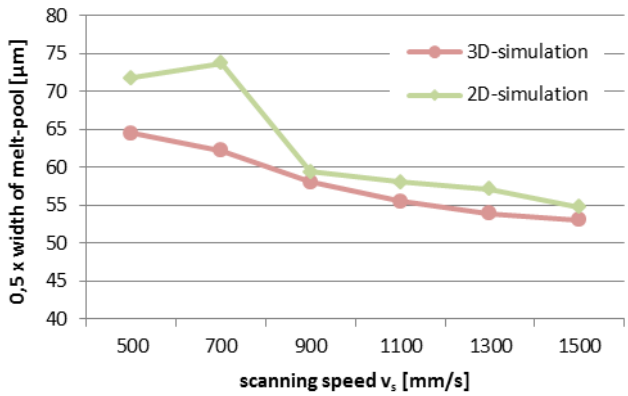

Fig. 3. Comparison of the size of the melt-pool for the 2D- and 3D-simulation of a laser beam scanning over bulk material of TiAl6V4 for different scanning speeds v_s with a constant laser power of P_L=180 W

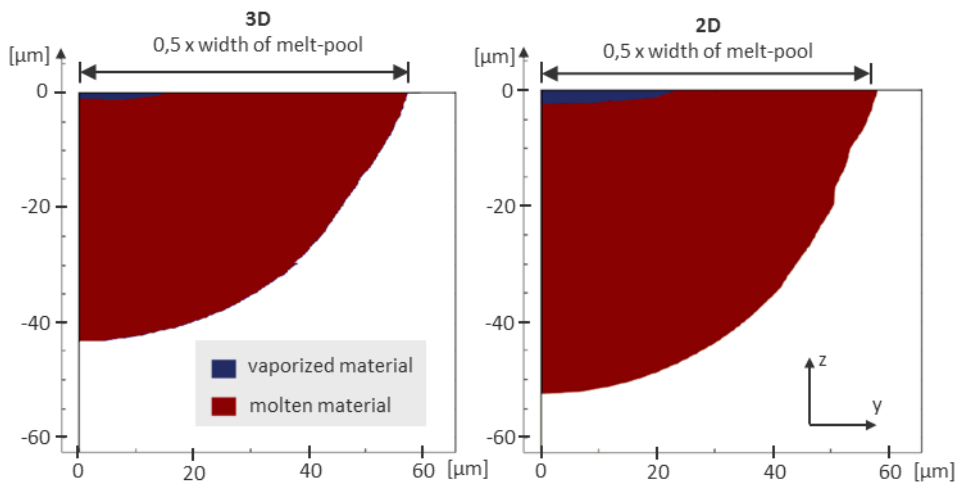

Fig. 4. Comparison of melt-pools for 2D- and 3D-FEM simulation for a scanning speed of 900 mm/s and laser power of P_L=180 W

2.2. Description of the 2D-FEM model

To be able to simulate the effect different laser beam intensity profiles have on the SLM process, it is essential to accurately implement all important physical phenomena and material properties. During the process, the laser beam interacts with the powder layer on top of a solid material as a volumetric heat source, because of the porous structure of the powder. When the material is molten and solidified, the optical penetration is close to zero and the energy of the laser beam has to be modeled as a surface heat source.

The developed FEM model focuses on simulating the thermal behavior during the melting of the powder material close to the interaction zone of the laser beam. Therefore the equation of heat conduction according to Fourier is calculated for each time step. Since radiation and convection is known to have very little effect they are not considered as in Roberts et al., 2009, and Niebling et al., 2002. Furthermore a mechanical simulation and motion of material are also neglected.

The powder material is simulated as a bulk material. To replicate the thermal properties of powder, the density as well as heat capacity of the solid material is multiplied by the packing density φ of the powder material (refer to table 2). This method has been proven to accurately represent the thermal behavior of metal-powder by Roberts at al., 2009. The heat conduction is defined with 1% of the corresponding value of solid material due to a very small contact surface of the powder particles as in Gusarov et al., 2009.

For the simulation, a 2D-model consisting of two domains was implemented into COMSOL Multi-physics 4.4, refer to figure 5. Domain A has a mesh size of 5 µm to accurately simulate the interaction of the laser beam with the material. In domain B the mesh is coarsened with distance from the interaction-zone to reduce computation time. Since only a single track on top of bulk TiAl6V4 material is simulated, a symmetry condition is used. To simulate a moving laser beam, a time-dependent energy input is implemented inducing thermal energy in the top layers, as shown in figure 5. The different heat input mechanisms for powder, liquid and solid material are considered by a switch function. At the beginning of the simulation, domain A has material properties of powder and the energy is applied as a volumetric heat source. When the temperature of the top-node of each column of nodes once surpasses the melting temperature, the energy is applied as a surface heat source for the liquid and solid state.

Since qualitative results are sufficient for the first investigations, a mechanical simulation, flow of molten material as well as forming of the melt-pool due to surface tension and the Marangoni effect are not considered. This would increase the complexity of the model and significantly increase the computation time.

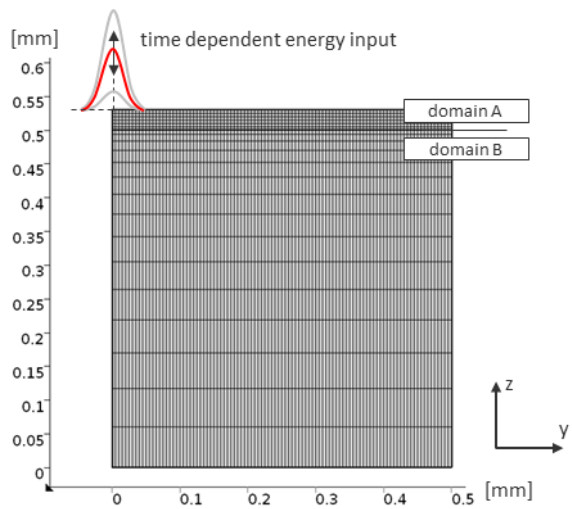

Fig. 5. Basic setup of the 2D-FEM model

Table 2. Data for the 2D-FEM model used for the simulation

Data for the simulation	Values	Unit
Size of model	530 x 500	µm
Mesh size domain A	5	µm
Laser beam radius r_b	45	µm
Layer thickness of powder bed	30	µm
Packing density of powder material φ	60	%

2.3. Material Properties

All important material properties (conductivity, heat capacity, absorptivity, density, …) depend on the material state (powder, liquid, solid, …) as well as on the temperature. Particularly for the liquid and powder state, the literature shows significant variance in the property-values. For the liquid phase, the material properties are hard to measure, as shown in Gonzales et al., 2012, and for powder material they are highly depending on the actual state of the material like particle size distribution or surface roughness as shown by Bergström, 2008.

For the developed model the material properties defined by Mills, 2002, were chosen, since they show one of the most complete sets of data for bulk and liquid TiAl6V4. To complete the data up to a temperature of 2800 K, data from Boivinieau et al., 2006, have been added. The latent heat of fusion is considered by the effective heat capacity method as in Heim, 2005. Since vaporization of the material is not implemented in the model, the temperature of each node must not exceed the evaporization temperature in order to maintain the temperature gradients in the model at a realistic level. Therefore the heat capacity at the evaporization temperature is increased rapidly.

The actual data for the thermal properties are shown in figure 6. For the simulation the values are smoothened to reduce computation time and numerical issues occurring in FEM with rapidly changing parameters. Absorptivity values used for the simulation are shown in table 3.

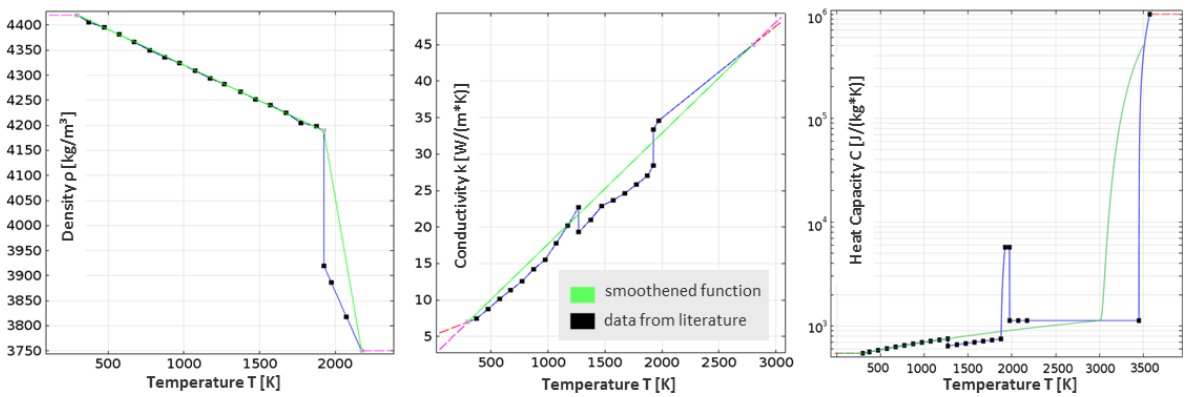

Fig. 6. Conductivity, density and heat capacity of TiAl6V4 in solid, liquid and gaseous state used for the simulation. Data taken from Mills, 2002 and Boivinieau et al., 2006. In green, the smoothened functions are shown, used for the simulation.

Table 3. Values for absorptivity used in the simulation for powder, liquid and solid TiAl6V4

Absorptivity	Value	Unit	Reference
Powder TiAl6V4	40	%	Klocke et al., 2003
Liquid TiAl6V4	40	%	Boivinieau et al., 2006
Solid TiAl6V4	20	%	Gonzales et al., 2012

2.4. Experimental validation of the 2D-FEM model

For the validation of the 2D-FEM model, solid blocks of TiAl6V4 were manufactured in SLM with single tracks of different scanning speeds on top, as shown in table 4 and figure 7. Cross sections of the

manufactured specimen were produced, and the area of molten powder material was measured and compared to the area of molten powder material in the simulation. To compensate for measurement inaccuracies and variance in the process, three different tracks were measured for each parameter set.

The specific shape of the melt-pool of the simulation, as seen in figure 7 (c), has also been observed by Yushanov, 2014, and Varquez et al., 2012. It can be explained by the neglection of material flow in liquid phase as well as the very low conductivity of the powder, leading to a heat accumulation in the powder bed.

Table 4. Parameters used for experiments and simulation of melting of single track of TiAl6V4 powder on top of solid TiAl6V4-material

Parameters for Experiments	Values	Unit
Laser Power P_L	180	W
Scanning Speed v_s	500, 700, 900, 1100, 1300, 1500	mm/s
Intensity Profile	Gaussian	

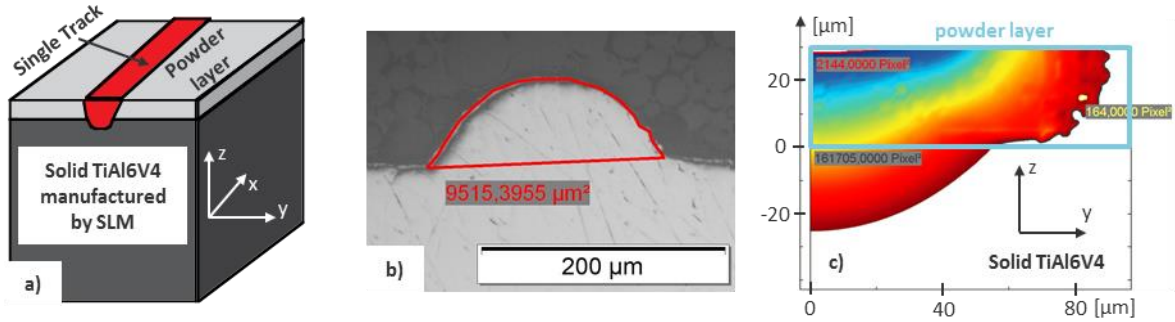

Fig. 7. (a) sketch of experimental set-up; (b) measured area of single track for scanning speed of v_s=900 mm/s and laser power of P_L=180W; (c) results from simulation: in color the material above melting temperature is shown for one half of the single track due to symmetry condition used in the model. For verification, the area of material above melting temperature in the powder layer was measured.

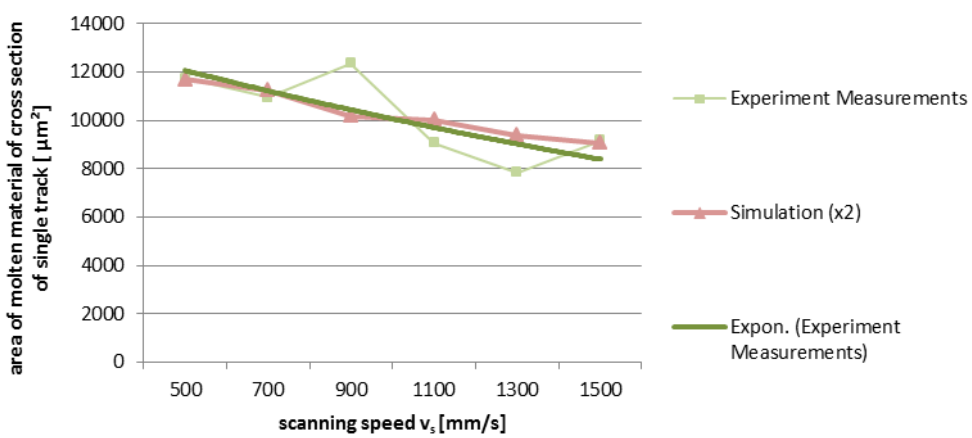

Fig. 8. Area of molten powder material for experiments and 2D-FEM simulation at different scanning speeds and a laser power of P_L=180 W. For the results of the experiments, an exponential trend line is shown. The area of the results of the simulation is multiplied by a factor of two to visualize qualitative agreement.

The results in figure 8 show a very good qualitative agreement between the simulation and the experiment, although the actual values of the simulation are half as big as the values for the experiments. This is can be explained by the neglaction of mechanical simulation in the model. Material flow in the liquid phase as well as melt-pool forming due to surface tension and the Marangoni effect will enhance the heat distribution in the powder layer and increase the size of the melt-pool.

Nevertheless, the developed model is very well-suited for qualitative analysis of the effect of different laser beam intensity profiles on the energy input and heat distribution, due to its low complexity and good qualitative agreement with the experiments.

3. Results of the simulation

To get a first impression on how the energy input and heat distribution can be optimized by different laser beam intensity profiles, the size of the melt-pool was calculated for three different profiles at different laser powers and scanning speeds, shown in table 5. Next to a Gaussian laser beam intensity profile, two different variations of donut-shaped profiles were simulated, shown in figure 9.

In figure 10, the area of molten powder material is shown for the three different laser beam intensity profiles for different laser powers and scanning speeds. It can be seen, that the size of the melt-pool for the Gaussian laser beam intensity profile is significantly lower, than the size of the donut-shaped intensity profiles for all sets of parameters. This indicates that donut-shaped intensity profiles are capable of increasing the energy-efficiency of the process and can optimize the energy input.

Table 5. Scanning parameters used for the simulation

Parameter	Values	Unit
Laser power P_L	200, 250, 300	W
Scanning speed v_s	1000, 1250, 1500	mm/s

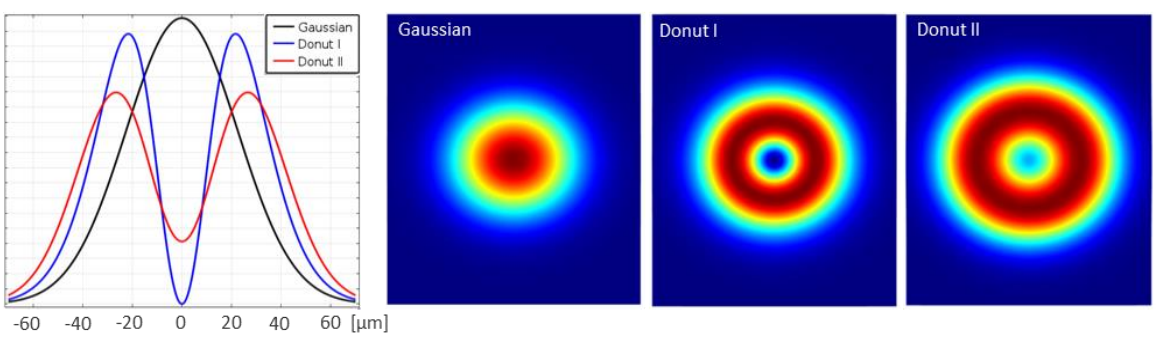

Fig. 9. Different laser beam intensity profiles used for the simulations

To confirm this assumption, melt-pools of comparable size for each laser beam intensity profile are shown in figure 11. In table 6 the corresponding parameters are listed. It can be seen, that for a Gaussian laser beam intensity profile the amount of energy necessary to obtain this melt-pool size (0,24 J/mm) is almost double as high as the corresponding energy input of the donut II profile (0,13 J/mm). Additionally, the area of powder material exceeding the vaporization temperature is significantly higher for the Gaussian profile. During the process, the vaporized material can interact with the laser beam and destabilize the melting-

process. Therefore, an optimized laser beam intensity profile might lead to a more robust SLM process. Furthermore, it can be seen that the scanning speeds and melting rates for the donut shaped laser beam intensity profiles are higher. In combination with a lower amount of vaporized material, this indicates that a productivity increase is possible with optimized laser beam intensity profiles.

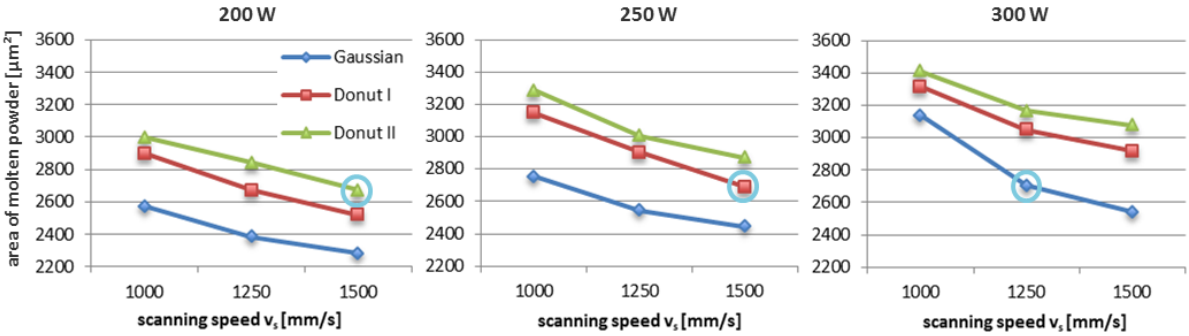

Fig. 10. Area of molten powder material in the simulation for different laser beam intensity profiles, scanning speeds and laser powers

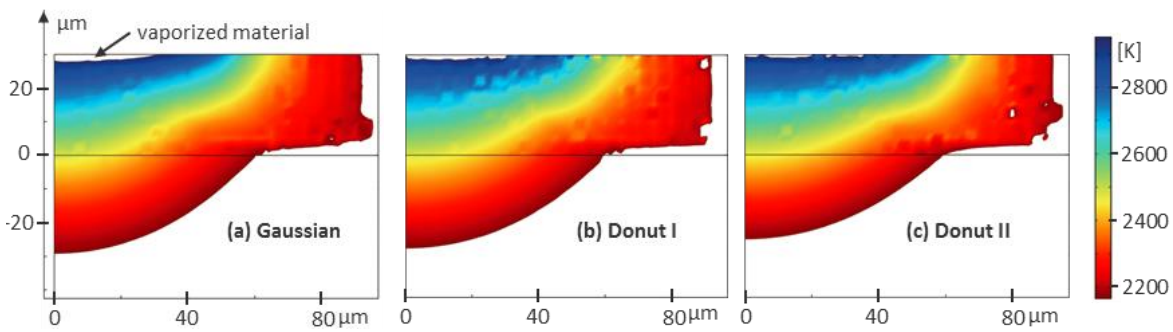

Fig. 11. Graphs of melt-pools of approximately same size for different laser beam intensity profiles (a) Gaussian intensity profile, P=250 W, v_s=1250 mm/s; (b) Donut I intensity profile, P=250 W, v_s=1500 mm/s; (c) Donut II intensity profile, P=200 W, v_s=1500 mm/s

Table 6. Comparison of the energy input, area of vaporized material and melting rate of different laser beam intensity profiles for approximately same area of molten powder material.

	Gaussian	Donut I	Donut II
Laser power P_L [W]	300	250	200
Scanning speed v_s [mm/s]	1250	1500	1500
Energy input [J/mm]	0,24	0,17	0,13
Area of vaporized material [µm²]	64	36	18
Melting rate [mm³/s]	3,4	4,0	4,0

4. Conclusion and Outlook

The results show that donut-shaped laser beam intensity profiles are capable of optimizing the energy input and heat distribution in the SLM process. Due to a more uniform energy input, the energy efficiency of

the process can be increased and vaporization of material can be avoided, which will contribute to a more robust process. Furthermore, an increase in productivity of the SLM process is likely, due to higher melting rates of the donut shaped laser beam intensity profiles at the same energy input.

In a next step, the 2D-FEM model should to be optimized to be able to predict the actual size and shape of the melt-pool quantitatively. Therefore, a mechanical simulation has to be included to be able to account for shrinkage due to the porosity of the powder, flow of molten material, forming of the melt-pool due to surface tension and the Marangoni effect. Furthermore, vaporization of material should be considered by extraction of energy and critical material properties like absorptivity should be defined more accurately.

With the improved FEM model, it will be possible to simulate the actual shape of the melt-pool for different laser beam intensity profiles, which will help to find the optimal laser beam profile for the process. For the verification of the results, experiments with a beam shaping optic in an SLM machine should be conducted.

References

Wohlers Report 2014: 3D Printing and Additive Manufacturing State of the Industry - Annual Worldwide Progress Report, Wohlers Associates, 2015.

Giuliani, V., Hugo, R. J., Gu, P., 2009. Powder Particle Temperature Distribution in Laser Deposition Technologies, Rapid Prototyping Journal Bd. 15, Nr. 4, p. 244.

Wellburn, D., Shang, S., Wang, S. Y., Sun, Y. Z., Cheng, J., Liang, J., Liu, C. S., 2014. Variable Beam Intensity Profile Shaping for Layer Uniformity Control in Laser Hardening Applications. International Journal of Heat and Mass Transfer Bd. 57, p. 189-200.

Zeng, K., Pal, D., Stucker, B., 2012. A Review of Thermal Analysis Methods in Laser Sintering and Selective Laser Melting, p. 796.

Zaeh, M., Branner, G., 2009. Investigations on Residual Stresses and Deformations in Selective Laser Melting, Production Engineering Bd. 4, p. 35.

Song, B., Dong, S., Liao, H., Coddet, C., 2011. Process Parameter Selection for Selective Laser Melting of TiAl6V4 based on temperature distribution simulation and experimental sintering, The International Journal of Advanced Manufacturing Technology Bd. 61, p. 967.

Cloots, M., Spierings, A., Wegener, K., 2013, Thermomechanisches Multilayer-Modell zur Simulation von Eigenspannungen in SLM-Proben, Tagungsband Schweißen und Wärmebehandlung, p. 59.

Vansteenkiste, G., 2012. Comparison of numerical modelling of the Selective Laser Melting, Engineering Materials, p. 3.

Gusarov, A. V., Yadroitsev, I., Bertrand, P., Sumrov, I., 2009. Model of Radiation and Heat Transfer in Laser-Powder Interaction Zone at Selective Laser Melting, Journal of Heat Transfer Bd. 131, p. 072101.

Roberts, I. A., Wang, C. J., Esterlein, R., Standford, M., Mynors, D. J., 2009. A Three-Dimensional Finite Element Analysis of the Temperature Field during Laser Melting of Metal Powders in Additive Manufacturing, International Journal of Machine Tools and Manufacture Bd. 49, p. 916.

Niebling, F., Otto, A., Geiger, M., 2002. Analyzing the DMLS-Process by a Macroscopic FE-Model, Proceedings of 13th Solid Freeform Fabrication, p. 384.

Gonzales-Fernandez, L., Risueno, E., Perez-Saez, R. B., Tello, M. J., 2012. Infrared Normal Spectral Emissivity of Ti-6Al-4V Alloy in the 500-1150K temperature range, Journal of Alloys and Compunds Bd. 541, p. 144.

Bergström, D., 2008. The Absorption of Laser Light by Rough Metal Surfaces, Journal of Applied Physics Bd. 103 p. 103515.

Mills, K. C., 2002, Recommended Values of Thermophysical Properties for Selective Commercial Alloys, Cambridge: ASM International & Woodhead Publishing Limited.

Boivineau, M., Cagran, C., Doytier, D., Eyraud, V., Nadal, M.-H., Wilthan, B., Pottlacher, G., 2006. Thermophysical Properties of Solid and Liquid Ti-6Al-4V (TA6V) Alloy, International Journal of Thermophysics Bd. 27, p. 507.

Heim, D., 2005. Two Solution Methods of Heat Transfer with Phase Change, International Ninth Conference Ibpsa, p. 397.

Klocke, F., Wagner, C., Ader, C., 2003. Development of an Integrated Model for Selective Metal Laser Sintering, Proceedings of the CIRP International Seminar on Manufacturing Systems, p. 387.

Yushanov, S., Crompton, J.S., Koppenhoefer, K. C., 2014. Thermal Analysis of Additive Manufacturing, COMSOL Conference 2014 Bosten, p.1.

Varquez, F., Ramos-Grez, J. A., Walczak, M., 2012. Multiphysics Simulation of Laser-Material Interaction during Laser Powder Deposition, International Journal of Advanced Manufacturing Technology Bd. 59, p. 1037.